# DEVELOPMENT OF A SIMULTANEOUS CRYO-ANCHORING AND RADIOFREQUENCY ABLATION CATHETER FOR PERCUTANEOUS TREATMENT OF MITRAL VALVE PROLAPSE

By

Steven Michael Boronyak

Thesis

Submitted to the Faculty of the

Graduate School of Vanderbilt University

in partial fulfillment of the requirements

for the degree of

MASTER OF SCIENCE

in

Biomedical Engineering

May, 2012

Nashville, Tennessee

Approved:

W. David Merryman, Ph.D.

Robert L. Galloway, Ph.D.

ACKNOWLEDGEMENTS

First, I would like to thank Dr. David Merryman for his guidance and support throughout the last two years. Second, I would like to thank my fellow lab members for making work more fun than it needs to be. Third, this work was funded by the Wallace H. Coulter Foundation, and I thank them, too. Cheers.

TABLE OF CONTENTS

LIST OF FIGURES

# CHAPTER I

## INTRODUCTION

### Background

*Mitral Valve Anatomy and Function*

The mitral valve (MV) is a bi-leaflet heart valve which sits between the left atrium and left ventricle of the heart. The complex anatomy of the MV consists of five primary components: (1) the annulus, a fibrous ring of tissue located at the base of the atrium, (2) two leaflets, consisting of the anterior and posterior leaflets, (3) commissures, which are the sites of separation between the leaflets, (4) chordae tendineae, which act to tether the free edges of the MV leaflets to the ventricular wall, and (5) the papillary muscles, the sites of chordae tendineae attachment (Fig. 1). The anterior leaflet is the larger of the two leaflets, and is approximately twice the height of the posterior leaflet.[14] The posterior leaflet consists of three distinct scallops, with the central scallop being the largest in approximately 90% of normal hearts.[14]

During normal functioning of the heart, the MV opens during diastole in order to allow passive filling of the left ventricle. During systole, when the heart is pumping blood to the systemic circulation of the body, the MV is closed and must resist large pressures (>120 mmHg) exerted on it to prevent reverse blood flow. Abnormalities of any of the primary components of the MV, as well as problems associated with left atrial or left ventricular dysfunction, can lead to malfunctioning of the MV,[32] and the type and severity of the diseased structure determines whether surgical techniques are needed to treat the defect.

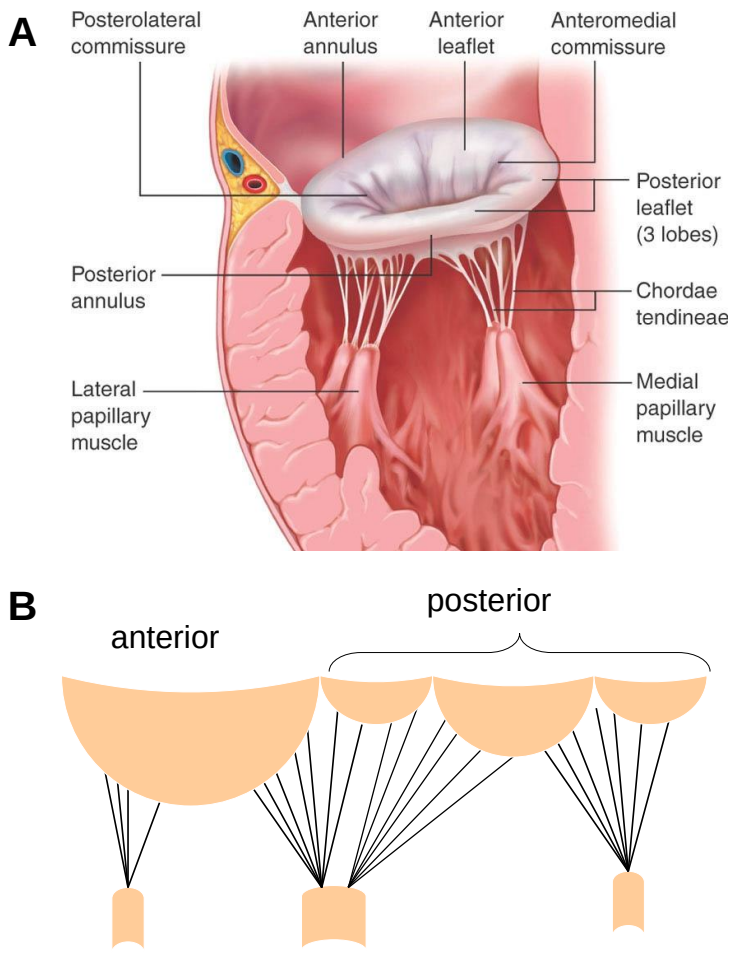


**Figure 1. Mitral Valve Anatomy.** A) Anatomy of the mitral valve, indicating the five major strutural components: the annulus, leaflets, commisures, chordae tendineae, and papillary muscles. B) A comparison of the larger, anterior leaflet and the three scallops that form the posterior leaflet. *Figure A from Otto*.[35]

*Mitral Regurgitation and Mitral Valve Prolapse*

Problems associated with the MV result in a "leaky" valve, in which reverse blood flow occurs across the MV during systole. This is termed mitral regurgitation (MR), and severe cases of MR can lead to left ventricular dysfunction and congestive heart failure.[41] Poor leaflet coaptation is the endpoint through which MR occurs, and one specific syndrome is termed mitral valve prolapse (MVP), which affects about 2% of the

population[13] and is defined as superior displacement greater than 2 mm of one or both leaflets into the atrium during systole (Fig. 2).[26] MVP can be characterized by any of the following conditions: thickened and redundant leaflets, annular dilatation, and thickened and elongated chordae tendineae.[14] The severity and underlying cause of MR due to MVP dictates the type of treatment administered, and open-chest replacement or repair is the current gold standard for treatment of moderate-to-severe and severe MR in patients with symptoms of left ventricular dysfunction.[10] This represents a significant problem in older patients who are more at-risk when undergoing invasive surgical procedures, a population that is currently growing, as the population of Americans aged 65+ is estimated to more than double – from 34 to 79 million – over the next 50 years.[45]

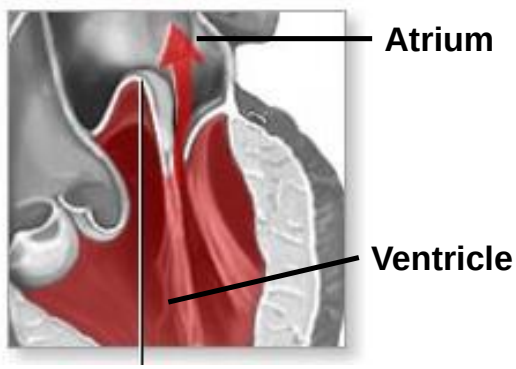


**Figure 2. Mitral Valve Prolapse.** Superior displacement of mitral valves into the left atrium during systole results in mitral regurgitation. Mitral valve prolapse can affect one or both leaflets, and is shown affecting the anterior leaflet above. *Figure from Medline.*[1]

*MVP Due to Degenerative MR*

The most common cause of MVP is due to a degenerative disease of the MV apparatus termed myxomatous MV disease, and an estimated 1% to 2% of the population has some form of myxomatous MV disease.[9] Additionally, approximately 6.5% to 9% of all diagnosed cases of MVP result in severe MR,[8,12] requiring treatment to improve quality of life. While myxomatous disease is currently not well understood at the

cellular and molecular levels,[9] it is well characterized at the tissue and functional levels. Histology of autopsied leaflets with myxomatous disease indicates disrupted and fragmented collagen architecture with a larger than normal layer of proteoglycans (Fig. 3).[37] These tissue level changes cause MV leaflets with myxomatous disease to become thickened and enlarged, and the redundant tissue of these leaflets leads to poor leaflet coaptation and MR.

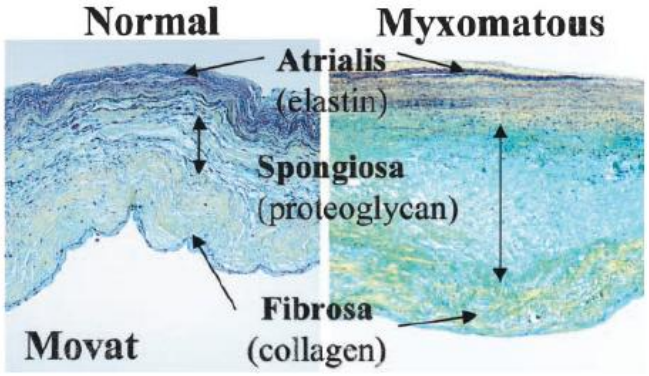


**Figure 3. Histology of Normal and Myxomatous Mitral Valve Leaflets.** Histology reveals fragmented collagen architecture and an increased quantity of proteoglycans in the myxomatous leaflet, shown left. *Figure from Rabkin et al*.[37]

Morphologic analysis of myxomatous MVs has shown a greater than two-fold increase in valve surface area, due to significant increases in both the anterior and posterior leaflet surface areas.[25] Additionally, the structural elements of the MV – collagen, elastin, and proteoglycans – constitute approximately 85-95% of leaflet dry weight,[7,28] indicating that alteration of these components will significantly affect leaflet mechanical properties. Myxomatous leaflets have previously been shown to be more extensible and less than half as strong as normal leaflets, further contributing to leaflet prolapse and MR.[5] Similar enlargement and extensibility changes can also occur in the chordae tendineae, in which the chords become thickened and elongated, leading to

leaflet billowing into the atrium during systole. It is the combination of (1) increased surface area and (2) increased mechanical compliance that leads to prolapse of myxomatous leaflets during systole. Due to the redundant leaflet surface area present in enlarged, myxomatous leaflets, the coaptation surface, or closing edge, cannot form a smooth seal, leading to MR (Fig. 4). Depending on the severity and extent of the disease, both the MV leaflets and chords can be affected separately or in combination. Thus, treatments to repair the MV to mitigate MR due to myxomatous disease are focused on improving leaflet coaptation via repair of the leaflets or alteration of the chordae tendineae.

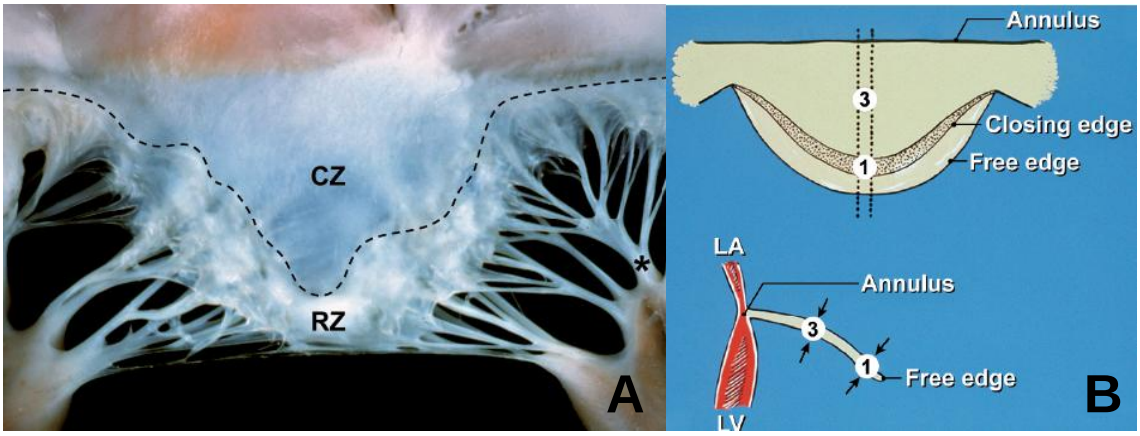


**Figure 4. Mitral Valve Closing Edge.** The closing edge of the MV leaflet lies close to the free edge of the leaflet, just below the clear zone (CZ). *Figure from Hurst's the Heart.*[14]

*Repair of the MV Due to Degenerative MR*

The current standard in long-term treatment of MVP due to myxomatous disease is open-chest surgical repair or replacement, depending on the severity and structure affected. To date, there are no known therapies that directly affect the disease process in the MV apparatus.[35] Repair of the MV is generally preferred over replacement due to lower rates of thromboembolism, resistance to endocarditis, the avoidance of a

prosthetic valve and associated long-term anticoagulation therapy, as well as the excellent durability of repairs – as long as 25 years – compared to valve replacement.[9] The benefit of MV repair is that it preserves the sub-valvular apparatus, consisting of the chords and papillary muscles, as removal of these structures has been associated with detrimental effects on left ventricular shape and performance.[19,46] However, recent rates of repair in those who required MV surgery were as low as 44% in the United States,[39] indicating that the complexity of valve repair makes treatment difficult, and more improved techniques will be necessary to improve repair rates.

Recently, less-invasive, percutaneous techniques have been in development to treat MVP. Percutaneous techniques are often preferred over surgical procedures because they have been shown to reduce the need for blood transfusions, decrease rates of infection, and reduce recovery time.[15,43] These benefits have the potential to reduce procedure cost and recovery time dramatically. Currently, the MitraClip (Abbot Laboratories) is the most developed of the percutaneous techniques in clinical trials.[4,11] The MitraClip is a percutaneous variation of the Alfieri edge-to-edge repair,[3] in which the two leaflets of the MV are sutured together, forming a double-orifice. The MitraClip allows this procedure to be performed percutaneously with the placement of a clip to pinch together the anterior and posterior leaflets. A recent comparison to open-heart MV repair indicated that while the rate of major adverse clinical events was significantly lower with the percutaneous treatment, the efficacy of treatment was also significantly lower than the open-heart repair.[10] Additionally, this procedure requires permanent placement of a foreign body and the long-term fluid dynamics of the double-orifice MV are poorly understood.[23] In combination with the results from the clinical trial, this indicates that there is still a need for additional percutaneous procedures that can reduce MR and preserve the MV apparatus.

*Percutaneous Application of Radiofrequency Ablation to Treat MVP*

One potential percutaneous treatment option for MVP is with radiofrequency ablation (RF), an established technique for treating cardiac arrhythmias that has been around since the mid-1980s. RF ablation utilizes electrical signals at around 300-700 kHz in order to generate resistive heating for ablation of tissue. It is dependent on power, electrode-tissue interface temperature, electrode size, and contact pressure.[21] The target of RF ablation is the collagen architecture of the MV leaflets, which contributes to much of the strength and mechanical properties of the tissue.[18] In MV leaflets, collagen is preferentially aligned with the circumference of the MV annulus, which causes an anisotropic loading response in normal leaflets (Fig. 5).

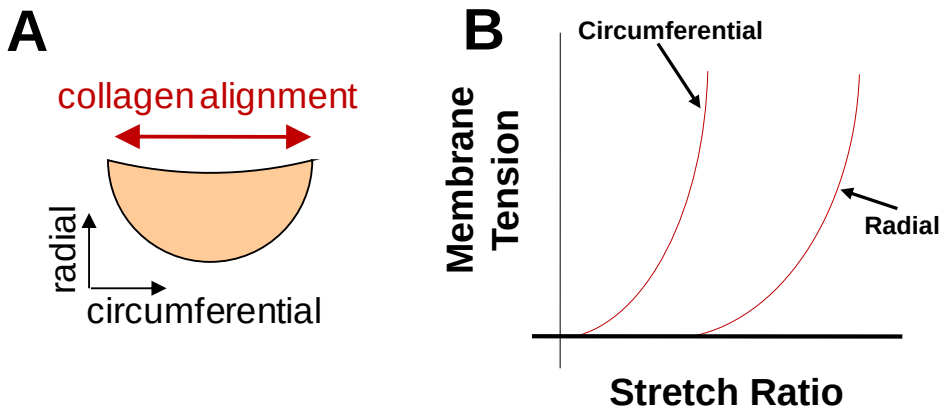


**Figure 5. Anisotropic Response of MV Leaflets.** A) Collagen is preferentially aligned with the circumferential direction in MV leaflets. B) Due to this collagen alignment, MV leaflets are more stiff in the circumferential direction than the radial direction.

This collagen alignment greatly affects the response of MV tissue to application of RF energy. Previously, the triple-helical structure of collagen has been shown to denature and contract when heated to greater than 65°C.[42] Following treatment with RF ablation, collagenous tissues undergo shortening in the direction of collagen alignment. Additionally, transmission electron microscopy has shown an increase in collagen fiber

diameter and a loss of cross-striations with increasing application of RF power.[33] Prior treatment of porcine MV leaflets with RF ablation *in vitro* has demonstrated directional length changes that are dependent on RF power (Fig. 6).[36] Therefore, the goal of using RF ablation to treat myxomatous MV leaflets is to induce permanent changes in leaflet geometry via resistive heating of collagen and subsequent shortening.

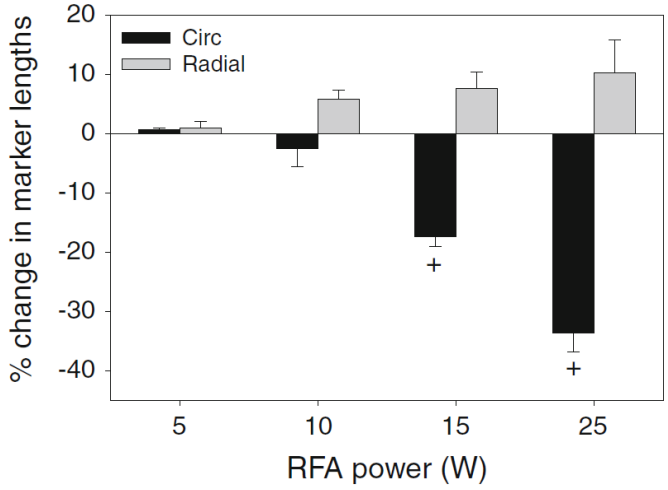


**Figure 6. MV Leaflet Geometry Following RF Ablation.** Change in length in the radial (grey bars) and circumferential (black bars) following 5, 10, 15, and 25 W of RF ablation. *Figure from Price et al*.[36]

The history of utilizing percutaneous application of RF ablation to alter the MV apparatus is brief and began with two animal studies published in 2008. The first of these studies used the QuantumCor device, which uses a circular RF ablation probe to reduce the MV annulus diameter and approximates an annuloplasty procedure used to treat some cases of MVP.[20] Use of the QuantumCor device in 16 sheep reduced the anterior-posterior dimension of the MV annulus by more than 20%, and these changes remained durable for the duration of the 180-day study, with tissue fibrosis and necrosis present at the endpoint.[16] However, this study was performed in normal sheep, with little to no traces of MR. The second study used a standard RF ablation catheter to apply RF

energy directly to MV leaflets in order to reduce leaflet size and alter biomechanical properties and was performed on two separate treatment groups.[43] The first group used RF ablation to directly treat myxomatous leaflets in beagles under open-heart surgery, resulting in 40-60% reduction in post-ablation MR. The second group applied RF ablation percutaneously to healthy beagles, until structural damage was observed, and monitored the durability of the changes for 6 weeks. The result of this study indicated that these changes are potentially durable long-term. While these results indicate that RF ablation is a feasible strategy for reducing MR in myxomatous MVs, percutaneous application of RF energy was difficult, due to the continuous movement of the MV leaflets. Thus, a strategy is needed to anchor the RF catheter tip, in order to move reliably apply RF energy directly to the leaflets themselves.

*Cryo-Anchoring for MV Attachment*

To date, no device has been published with the ability to temporarily anchor a catheter to a moving MV. In order to enable more reliable application of RF energy to MV leaflets, the requirements for an anchoring device are to enable reversible attachment to either the posterior or anterior MV leaflet, depending on the desired ablation target. Additionally, anchoring to the chords for RF ablation represents another potential target. Cryoablation is one technology that has been used to percutaneously treat cardiac arrhythmias since 1999,[24] which uses pressurized liquid nitrogen to cool a catheter tip to temperatures as low as -80°C. A technique termed cryo-mapping was developed for use with these cryoablation catheters, which cools the catheter tip to temperatures as low as -30°C to temporarily attach the catheter and induce electrophysiological changes in cardiac tissues.[21] This is performed with minimal cellular damage and little effect on the structural properties of the tissue.[40] Given the negligible amount of tissue damage induced at temperatures as low as -30°C, and the temporary,

reversible tissue attachment that can be created, this cryo-anchoring technique represents one potential strategy to maintain attachment to moving MV leaflets.

## Objective

The objective of this work was to develop and test a prototype catheter to determine the feasibility of radiofrequency ablation with cryo-anchoring in percutaneous treatment of mitral valve prolapse. One common cause of mitral valve prolapse is thickened and enlarged leaflets which billow back into the left atrium during valve closure, causing mitral regurgitation. The goal of this treatment strategy is to reduce mitral valve leaflet size via resistive heating with radiofrequency ablation in order to improve leaflet coaptation and reduce mitral regurgitation. However, in order to perform this procedure *in vivo*, a method is needed to provide attachment to moving mitral valve leaflets during administration of radiofrequency energy. Cryo-anchoring, which functions similarly to cryoablation, is one technique which can maintain this attachment. Cryo-anchoring utilizes liquid nitrogen to generate sub-freezing temperatures on the surface of a catheter tip, which provides adherence to tissues such as the mitral valve. Thus, the two techniques, radiofrequency ablation and cryo-anchoring, directly oppose each other and must be balanced in order to provide optimal treatment of mitral valve prolapse. The study that follows verifies the feasibility of utilizing these two techniques in close proximity, and provides an estimate for the amount of radiofrequency energy required to alter mitral valve leaflet geometry and biomechanics in the presence of cryo-anchoring.

## Specific Aims

1. Develop a catheter prototype that contains both a cryogenically cooled anchoring element (cryo-anchor) and a radiofrequency ablation electrode on the same catheter tip, capable of treating mitral valve leaflets *in vitro*
2. Quantify the effects of radiofrequency ablation treatment with cryo-anchoring on the geometry and biomechanical response of mitral valve leaflets.
3. Determine the mitral valve leaflet temperature distribution resulting from treatment with combined radiofrequency ablation and cryo-anchoring
4. Determine the attachment strength of the cryo-anchor to stationary mitral valve leaflets, both with and without radiofrequency ablation

# CHAPTER II

## MANUSCRIPT: DEVELOPMENT OF A SIMULTANEOUS CRYO-ANCHORING AND RADIOFREQUENCY ABLATION CATHETER FOR PERCUTANEOUS TREATMENT OF MITRAL VALVE PROLAPSE


### Abstract

Mitral valve prolapse is one subtype of mitral valve disease and is often characterized by enlarged leaflets that are thickened and have disrupted collagen architecture. The increased surface area of myxomatous leaflets with mitral valve prolapse leads to mitral regurgitation, and there is need for percutaneous treatment options that avoid open-chest surgery. Radiofrequency ablation is one potential therapy in which resistive heating can be used to reduce leaflet size via collagen contracture. One challenge of using radiofrequency ablation to percutaneously treat mitral valve prolapse is maintaining contact between the radiofrequency ablation catheter tip and a functioning mitral valve leaflet. To meet this challenge, we have developed a radiofrequency ablation catheter with a cryogenic anchor for attachment to leaflets in order to apply radiofrequency ablation. We demonstrate the effectiveness of the dual-energy catheter in vitro by examining changes in leaflet biaxial compliance, thermal distribution with infrared imaging, and cryogenic anchor strength. We report that 1250 J of radiofrequency energy with cryo-anchoring reduced the determinant of the deformation gradient tensor at systolic loading by 23%. Infrared imaging revealed distinct regions of cryo-anchoring and tissue ablation, demonstrating that the two modalities do not counteract one another. Finally, cryogenic anchor strength to the leaflet was reduced but still robust during the application of radiofrequency energy. These results indicate that a catheter having combined radiofrequency ablation and cryo-anchoring provides a novel percutaneous treatment strategy for mitral valve

prolapse and may also be useful for other percutaneous procedures where anchored ablation would provide more precise spatial control.

Key Terms

Heart valve mechanics, mitral valve prolapse, radiofrequency ablation, cryo-ablation, infrared thermal imaging

## Introduction

Mitral valve (MV) disease is the most common form of heart valve disease, occurring in approximately 2% of the population and resulting in 43,000 open-chest surgical procedures every year.[13] MV prolapse (MVP) is one subtype of the disease and is characterized by superior displacement of one or both leaflets into the left atrium, resulting in mitral regurgitation (MR). One common cause of MVP is myxomatous mitral valve disease, which is characterized by thickened and enlarged leaflets, disrupted and compromised collagen architecture, and an increased quantity of proteoglycans. The etiology is unknown at this time.[37]

The current gold standard to correct MVP is open-chest surgical valve repair or replacement, which is highly undesirable for elderly patients. In the past decade, percutaneous treatment of MV disease has received a great deal of interest.[6,9,31] Specifically, the MitraClip[4,11] (Abbott Laboratories) is one technique undergoing clinical trials and is a percutaneous variation of the Alfieri edge-to-edge technique,[3] which creates a double orifice valve by fixing together the free edges of the anterior and posterior leaflets. The MitraClip has been assessed in the EVEREST II clinical trial and was found to have a 55% rate of primary end point efficacy at 12 months, which included freedom from grade 3+ or 4+ MR, freedom from death, and freedom from surgery for MV dysfunction.[10] Additionally, major adverse clinical events occurred at a rate of only 15%

in the percutaneous-repair group at 30 days, compared with 48% of patients in the surgery group. While the reduced complication rate indicates that percutaneous strategies may represent a safer alternative to open-chest surgery, the end point efficacy indicates that there remains room for improvement. Therefore, we believe that there is a need for additional percutaneous options to treat MVP that preserve the MV apparatus and restore normal fluid mechanics.

One potential percutaneous treatment strategy for myxomatous MVP is the use of radiofrequency (RF) ablation to reduce MV leaflet size to reduce MR. Due to the increased size of myxomatous leaflets, they fail to properly coapt during systole, and this redundancy of excess leaflet tissue provides an opening for regurgitant flow. By reducing leaflet size, coaptation could improve and thereby reduce MR. RF ablation generates thermal lesions via resistive heating of tissue and is dependent on power, interface temperature, electrode size, and contact pressure.[21] For our purposes, the target of RF ablation is the disrupted or distended collagen architecture of the MV leaflets; collagen has been shown to denature and contract when heated to temperatures greater than 65°C.[42] Using biaxial mechanical testing, we have demonstrated that RF ablation effectively reduces MV leaflet geometry and alters biomechanical compliance *in vitro.*[36]

Previously, RF ablation treatment of myxomatous MVP has been shown to be feasible in a surgical canine model in which an acute *in vivo* study was performed on beagles with MR under open-heart surgery, demonstrating a mean 49.6% reduction in post-ablation MR.[43] Additionally, a chronic *in vivo* study was performed on healthy beagles to assess the ability to apply RF energy percutaneously and to assess the durability of the procedure at 6 weeks. An average of 22 applications of RF ablation for 60 seconds at an average power of 58 W was required to induce structural alteration of the leaflets, and alterations were found to be durable 6 weeks later. For comparison, 4 applications of RF ablation for approximately 40 seconds at a power of 16 W were

required to reduce MR in the acute *in vivo* study. These results indicate that: (1) RF ablation is a feasible technique for reducing MR, (2) the alterations due to RF ablation remain durable, although the effects on valvular tissues after 6 weeks are not known, and (3) more RF energy is required to induce structural alteration of MV leaflets when applying RF energy percutaneously due to heat dissipation to the surrounding blood. The primary explanation for the increased number of RF ablation applications in the percutaneous case is that poor contact exists between the RF electrode on the catheter tip and the surface of the moving MV leaflet. The result of this is that RF energy may have been delivered entirely into the blood or into the surrounding myocardium. Therefore, to reduce misguided application of RF energy and improve delivery directly into the MV leaflet tissue, a stability technique is needed to physically anchor the catheter tip to the leaflet surface.

One possible method of maintaining contact between the RF ablation catheter tip and the moving MV leaflet is using a catheter with a cryogenically cooled anchoring element, or a cryo-anchor. This technique works similarly to cryo-ablation, which uses pressurized liquid nitrogen to cool a catheter tip to temperatures as low as -80°C and has been utilized since 1999 as an alternative for treating cardiac arrhythmias.[24] Cryo-ablation is generally less destructive than RF ablation and has previously been shown to maintain the extracellular collagen matrix, without collagen denaturation or contracture related to thermal effects.[40] Further, permanent damage to myocardial tissues due to cryo-ablation has been shown to occur only at temperatures below -30°C,[21] making this temperature an excellent target for use in a cryo-anchor. While cryo-anchoring is used here as a method to adhere to MV leaflets, it may have broader applications in use as a stability technique for a variety of percutaneous procedures. For example, treatments that require the use of RF ablation in dynamic environments, such as treatment of

cardiac arrhythmias, could potentially benefit from using cryo-anchoring for catheter stability.

The purpose of this study was to determine the feasibility of using cryo-anchoring and RF ablation on the same catheter tip and to quantify the biomechanical and thermodynamic effects of RF ablation on porcine MV leaflets. We hypothesized that an RF ablation catheter that utilizes a cryo-anchor will effectively adhere to and alter MV leaflet geometry and compliance, reducing MV leaflet size at maximum systolic load. To test this hypothesis, we developed a catheter prototype containing both a cryo-anchor for attachment and stability and an RF electrode for ablation. To investigate the effects of using cryogenic temperatures and resistive heating in close proximity, we quantified changes in biaxial mechanical compliance of MV leaflets and used infrared (IR) thermal imaging to discern distinct thermal regions within the tissue. We also quantified the anchor strength of the cryo-anchor both with and without RF ablation. These data support our hypothesis that simultaneous cryo-anchoring and RF ablation effectively reduces MV leaflet size and compliance, while further demonstrating that cryo-anchoring and RF ablation can function effectively in close proximity on a single catheter tip.

## Materials and Methods

### *Catheter Prototype*

A 4 mm (12 French) diameter catheter prototype was developed containing both a cryogenically cooled anchor (cryo-anchor) and an RF ablation electrode (Figs. 7A and 7B). The cryo-anchor and RF electrode reside in-line on the catheter shaft and are separated by a 1 mm spacer, with the cryo-anchor on the most distal point of the catheter. Both the cryo-anchor and RF electrode are constructed out of hollow copper rod and are approximately 1.9 mm in length. The cryo-anchor is thermally connected via a solder joint to an inner copper rod containing a lumen which allows liquid nitrogen

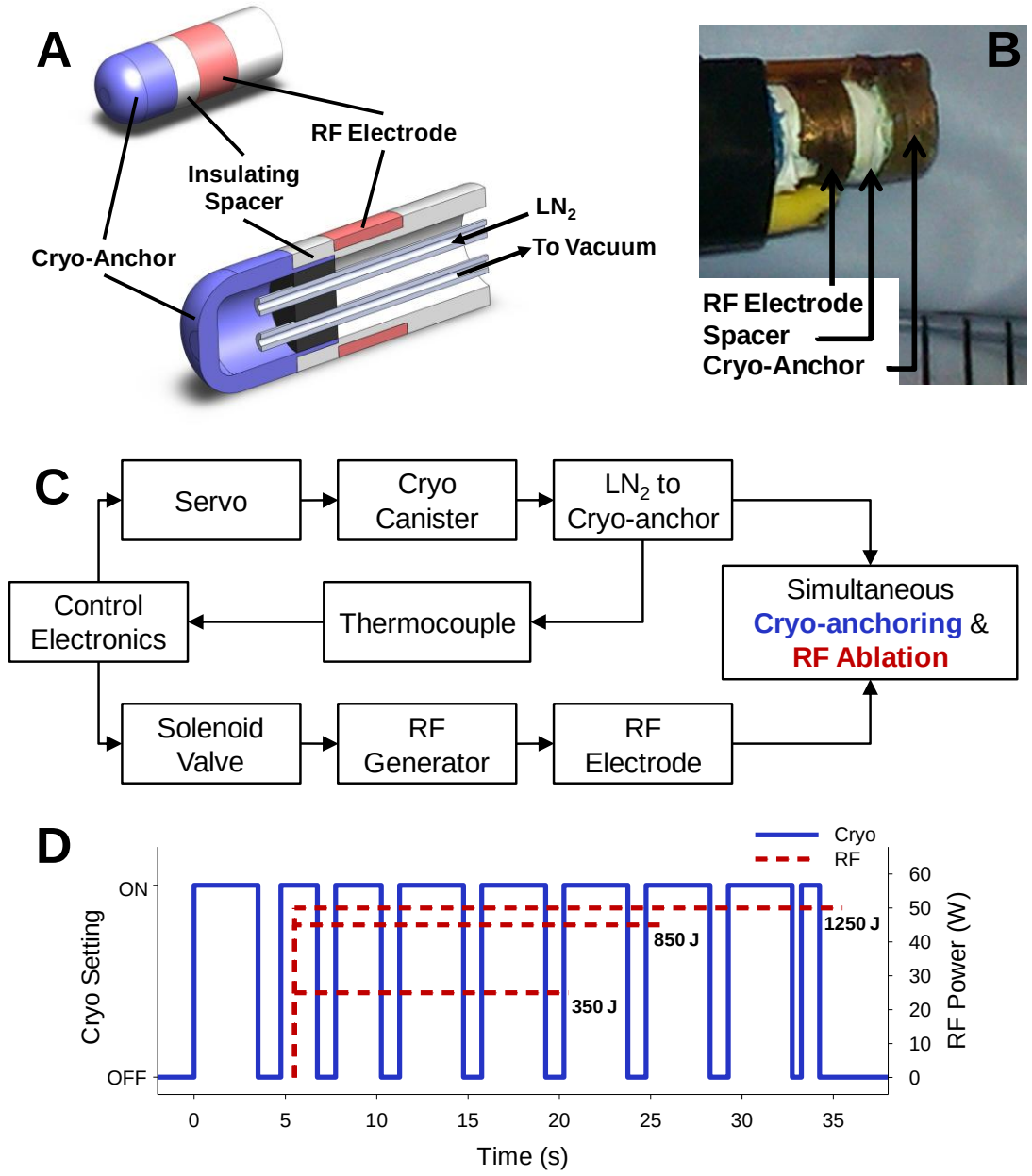


**Figure 7. RF and Cryo-Anchoring Catheter Design.** (A) Solid model cut-away of the catheter prototype design, indicating the relative positions of the cryo-anchor, insulating spacer, and RF electrode. (B) Catheter prototype tip used for all treatments of tissue (scale bar = 1/8"). (C) Flow chart representation of the control system used to integrate and synchronize cryo-anchoring with RF ablation for treatment of tissue. (D) Sequence programmed into the controller for performing RF ablation treatments with cryo-anchoring. Note that liquid nitrogen delivery to the catheter tip begins prior to RF ablation in order to first anchor the catheter tip to the tissue surface. RF power is represented as being applied instantaneously; however, it took ~3 s for RF power to reach target power. Final RF energy delivery (J=Joules) is indicated on the plot and represents total energy delivery of each treatment.

delivery. Teflon is used to insulate the RF electrode from the cryo-anchor and inner copper rod, and a thermocouple attached to the outer surface of the cryo-anchor records the temperature at the anchor-tissue interface. RF ablation is performed with an Osypka HAT 300 generator, capable of delivering a 500 kHz electrical signal at powers of up to 50 W to the RF electrode on the catheter tip. Liquid nitrogen is contained inside a handheld canister (Cry-Ac, Brymill Cryogenic Systems) and delivered to the catheter tip under vacuum by an inner lumen housed inside the catheter.

Control of RF ablation and liquid nitrogen delivery is performed via custom built control electronics for synchronization and repeatability (Fig. 7C). Liquid nitrogen flow control is binary, and a servo motor is used to switch flow on and off. The sequence used for liquid nitrogen flow was developed to anchor the catheter tip to the tissue sample prior to RF ablation and to maintain anchoring throughout the ablation (Fig. 7D). Control of the RF generator was performed by interfacing with the footswitch port on the generator, with air flow controlled by a solenoid valve and control electronics. For each ablation, one of three RF protocols was utilized at 25, 45, or 50 W of power for 15, 20, or 30 s, respectively (Fig. 7D). Due to the time required for the RF generator to increase the power to the desired set-point (~3 s), the total energy output was lower than that produced by the product of time and power (Joules = W s). The final energy delivery to the tissue, as recorded by the generator for each of the 25, 45 and 50 W ablations, was 350, 850, and 1250 Joules (J), respectively.

*Tissue Preparation*

Healthy porcine MV leaflets were obtained from a local abattoir (Hampton Meat Processing, Hopkinsville, KY), excised on-site, and frozen in phosphate buffered saline (PBS) at -20°C until testing. Anterior leaflets were chosen for the biomechanical and thermal imaging studies due to their larger and more continuous surface area compared

to posterior leaflets, although it is noted that posterior leaflets are more often affected by MVP.[9] The center portion of the leaflets were used and trimmed into rectangular sections (Fig. 8A) approximately 12 mm in the radial direction and 15 mm in the circumferential direction. The center portion was used as it experiences the most homogenous strains during MV closure.[38] For the anchor strength study, posterior leaflets were used for testing.

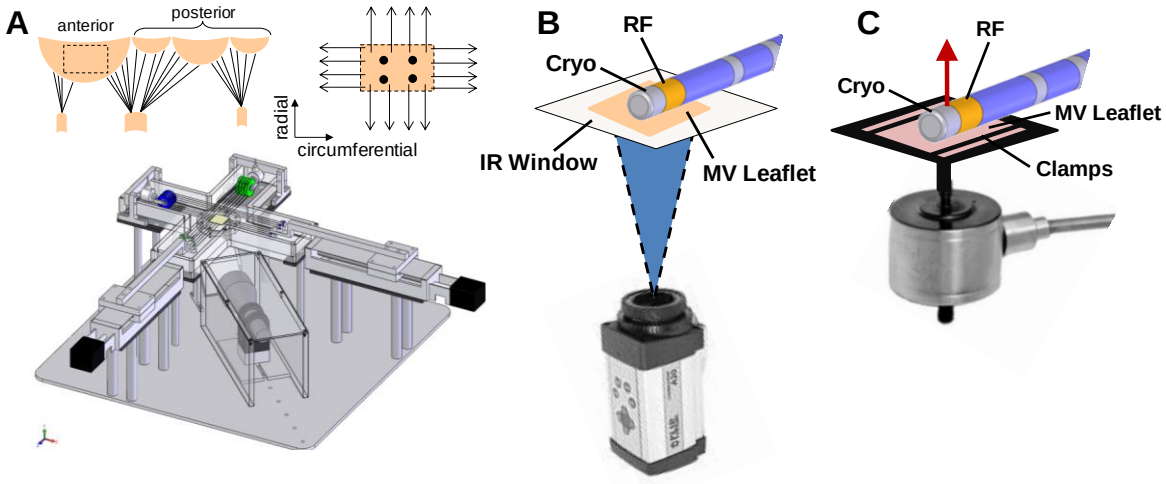


**Figure 8. Experimental Design.** (A) Mitral valve anatomy with marker placement and biaxial testing device with leaflet tissue in place. (B) Set-up for full thickness thermal imaging. The IR camera is placed below in order to measure the temperature distribution throughout the entire surface of the tissue. An IR window allows transmission of IR wavelengths for unimpeded temperature measurement. (C) Set-up for measurement of anchor strength of the cryo-anchor. Leaflets are clamped into the load cell assembly, and the maximum load is recorded.

*Biaxial Mechanical Testing*

Biomechanical analysis was performed using a custom-designed biaxial mechanical testing device (Fig. 8A).[36] Samples were loaded in each direction up to a membrane tension comparable to that experienced by the leaflet during systole (120 mmHg ≈ 90 N/m of membrane tension), and all testing was performed with samples fully submerged in PBS at 37°C. Prior to testing, each sample was pre-conditioned over ten loading cycles to 90 N/m with a 15 s rise time. Following pre-conditioning, a marker

reference was recorded and used as the unloaded state. Samples were then tested for ten cycles with a 15 s rise time to 90 N/m in order to determine untreated compliance. Stress-strain behavior has been found to be independent of loading rate for cycles with rise times of up to 15 s, thus tissues were not loaded at physiologic rates [17].

After determining leaflet biomechanical properties, samples were loaded to 10 N/m and subjected to one of the following four treatments with the catheter prototype. In order to determine the biomechanical effects of the cryo-anchor alone, samples were kept in contact with the cryo-anchor for 30 s at approximately -20 to -30°C (n = 3). To test the combined effects of cryo-anchoring and RF ablation, tissues were subjected to one of three treatment groups (n = 5) as described earlier and shown in Fig. 7D. During treatment, the fluid level in the bath was lowered to just below the surface of the sample in order to ensure that maximal energy transfer was through the tissue. By performing treatment such that all RF energy must pass through the sample, the amount of RF energy required to invoke the recorded biomechanical changes can be determined. The alternative is to completely submerge leaflets during treatment, but this provides a very low resistive path to ground, which bypasses the target tissue via direct conduction through the PBS bath. Four ground electrodes were placed in the bath, approximately 13 cm away from the tissue, to complete the electrical circuit for RF ablation. Following treatment, samples were returned to their unloaded state, a new marker reference was recorded to determine changes in unloaded geometry, and samples were loaded for ten cycles to 90 N/m. All data reported is from the tenth loading cycle of each experiment.

All analysis of biaxial mechanical data was performed using MATLAB (Mathworks). Marker positions recorded just prior to loading were used to determine geometric changes of the unloaded tissues due to treatment with the catheter prototype. Unloaded marker area was calculated as the area enclosed by the polygon connecting the four markers. Additionally, the percent change in the determinant of the deformation

gradient tensor, ***F*** (% change in det(***F***)) was used to provide a quantitative assessment of the biomechanical changes of the tissue at maximum systolic load. The determinant of ***F*** is the ratio of the deformed marker area to the marker area of the reference state, where:

$F_{11}$ and $F_{22}$ represent the stretch ratios in the circumferential and radial directions, respectively, and $\kappa_1$ and $\kappa_2$ provide a measure of shear. det(***F***) was determined at 90 N/m before and after treatment, and the unloaded marker reference state recorded just after pre-conditioning was used for all calculations. Because the same marker reference state is used to determine ***F*** in both the untreated and treated conditions, % change in det(***F***) provides a direct comparison of systolic leaflet deformation before and after treatment. Therefore, we refer to % change in det(***F***) at 90 N/m as % change in areal systolic deformation. In addition to reporting changes in det(***F***) due to treatment, we also report % change in axial systolic deformations which are changes in $F_{11}$ and $F_{22}$ at 90 N/m. For a more complete description of the calculation of ***F*** from biaxial mechanical testing, see Humphrey.[22]

*Infrared Thermal Imaging*

Thermal imaging of simultaneous cryo-anchoring and RF ablation was performed using an IR camera (ThermoVision A20M, FLIR Systems) with a measurement range of -20°C to 250°C and accuracy of ±2°C. Previous studies have used IR imaging to identify the lethal isotherm of RF lesions.[27,44] Leaflets were imaged in a custom built bath, and the camera was placed below the bath for imaging of full thickness changes in temperature distribution (Fig. 8B). An IR window (IR Material Window, Edmund Optics Inc.) was placed at the bottom of the bath to allow imaging through the bottom surface

by allowing transmission of IR wavelengths. Prior to treatment, an image was taken of a calibration phantom to determine the x and y distance scales. Testing was performed in PBS at room temperature, and the fluid level was lowered to just below the top surface of the tissue to allow maximal energy transfer through the leaflet. Four ground electrodes were placed in the bath in a circular pattern, each approximately 13 cm from the center of the leaflet. During ablation, a non-conductive plate was placed over the leaflet in order to maintain contact of the entire leaflet surface with the IR window. This was done to ensure that the temperatures measured were of the leaflet itself and not the fluid between the leaflet and IR window. All samples were then treated using one of the ablation sequences in Fig. 7D (n = 3 for each of the 350, 850, and 1250 J sequences), and images of the treatment were recorded at 1 Hz beginning at the onset of RF ablation using ThermaCAM Researcher software and synchronized with the ablation sequence using the control electronics. Images were then analyzed in MATLAB to produce thermal contour plots of the tissue. Additionally, the area of tissue heated to > 65°C was quantified in order to provide a measure of the extent of thermal contracture of the extracellular matrix collagen, and the tissue area < 0ºC was also quantified to provide an estimate of the attachment area of the catheter prototype.

*Anchor Strength*

In order to assess the anchor strength of the cryo-anchor both with and without RF ablation, a submersible load cell was used (Model 31 Mid, Honeywell). Posterior MV leaflets were clamped onto the load cell assembly and completely submersed in PBS at 37°C (Fig. 8C). Leaflets were completely submersed during treatment in order to test the anchor strength of the cryo-anchor in an environment that more closely mimics the *in vivo* case. The output from the load cell was amplified using a custom built amplifier circuit and read into LabView using a data acquisition card (NI 9205, National

Instruments). Anchor strength was tested at one of two protocols (n = 5 for each protocol). For the “Cryo Only” protocol, liquid nitrogen was pumped under vacuum to the catheter tip continuously for 10 s, and the catheter was then immediately pulled from the leaflet surface until separation. To determine the loss of anchor strength resulting from application of RF energy, the “RF + Cryo” protocol consisted of 5 s of continuous liquid nitrogen delivery, followed by 10 s of RF ablation at 50 W with continuous liquid nitrogen delivery. The catheter was then pulled away from the leaflet surface until separation. In both cases, the maximum load during separation was recorded. Maximum load was converted to anchor strength by dividing the load by 0.12 $cm^2$, the approximate area of the cryo-anchor in contact with the tissue.

*Statistics*

Data are presented as mean ± SE. To analyze significance of changes due to combined RF ablation and cryo-anchoring for the biomechanical and anchor strength studies, data were analyzed using a one way ANOVA ($\alpha = 0.05$) for multiple pair wise comparison (Holm-Sidak method).

## Results

*Tissue Geometry and Compliance*

Prior to treatment, leaflets displayed a typical, anisotropic mechanical response to loading,[18] with the radial direction much more compliant than the circumferential direction (Figs. 9A and 9B). This is due to collagen fibers being preferentially aligned in the circumferential direction. Following 30 s of cryo-anchoring, MV leaflets experienced negligible changes in geometry and mechanical response (Fig 9A). However, after 1250 J of RF ablation with cryo-anchoring, leaflets underwent significant changes. In the circumferential direction, changes in systolic deformation were attributable primarily to

shrinkage of the tissue, as indicated by a large shift in stretch ratio in the unloaded state (membrane tension = 0 N/m), while the radial direction underwent a decrease in systolic deformation with little geometric changes.

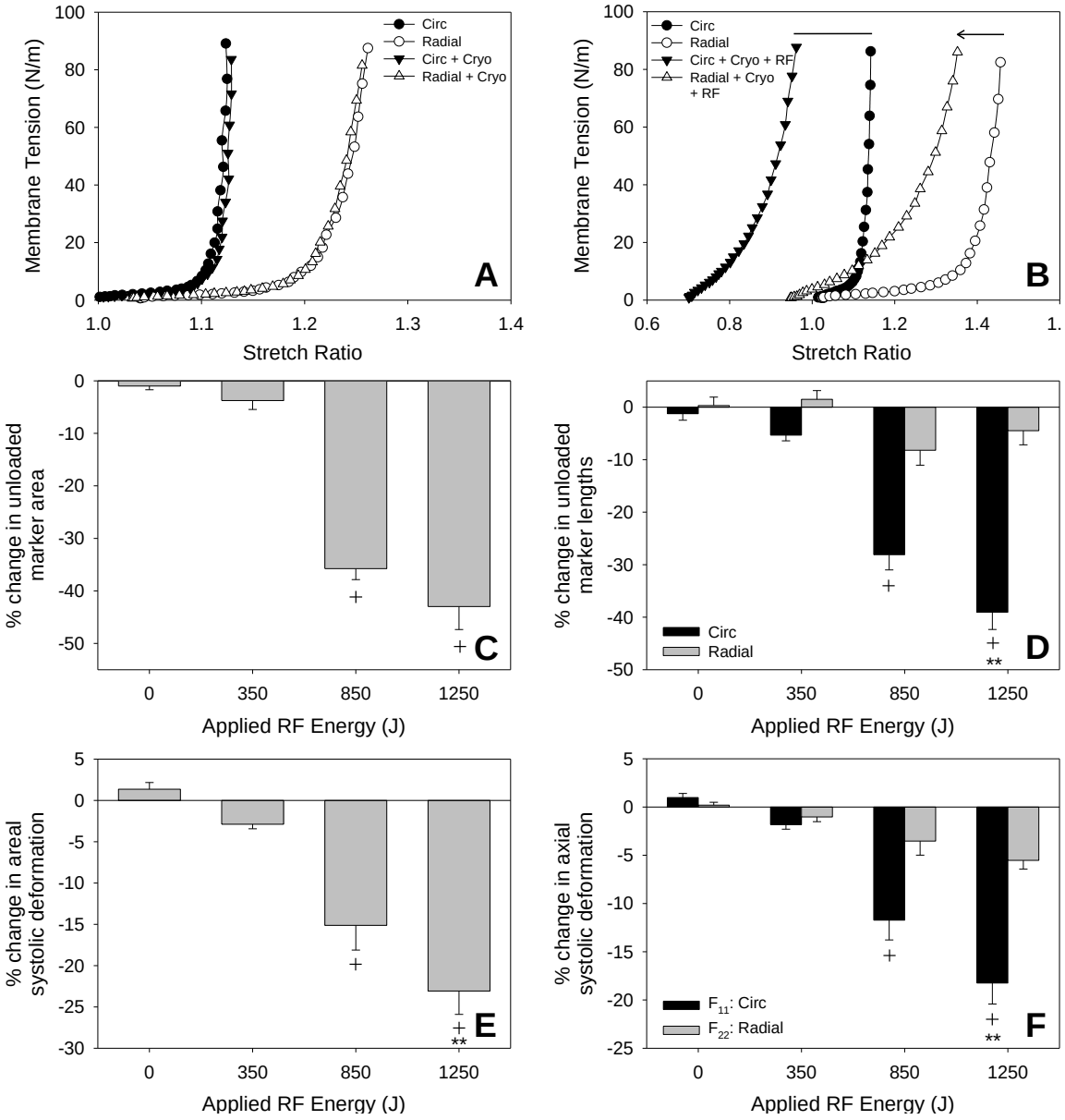


**Figure 9. Biaxial Mechanical Response.** Biaxial, membrane tension vs. stretch ratio following 30 s of cryo-anchoring without RF ablation (A) and with 1250 J of RF ablation (B). (C) % Change in unloaded marker area for each treatment group (0 J represents cryo-anchoring without RF ablation). % Change in unloaded marker lengths (D), areal systolic deformation (E), and axial systolic deformation (F) for each treatment group. $^{+}$ Significant decrease vs. 0 J ($p<0.001$) and $^{**}$ significant decrease vs. 850 J ($p<0.05$).

There was a consistent trend of decreasing marker area with increasing RF energy (Fig. 9C), due primarily to decreases in length in the circumferential direction (Fig. 9D). Change in systolic deformation was analyzed at maximum load, 90 N/m (Figs. 9E and 9F), with all deformations referenced to the marker reference state recorded just after pre-conditioning. Similarly to geometric changes, the areal systolic deformation decreased with increasing RF energy (Fig. 9E), due primarily to shrinkage in the circumferential direction. Additionally, there was a consistent trend of decreasing axial systolic deformation in both the circumferential and radial directions with increasing RF energy (Fig. 9F), although the changes in the radial direction were not significant.

*Temperature Distribution*

Leaflet tissue > 65°C was quantified to identify the area of the leaflet exposed to temperatures that cause thermal damage to collagen. The area > 65°C was found to increase with increasing RF energy, from 0.51 ± 0.13 $cm^2$ to 1.9 ± 0.13 $cm^2$ at energies of 350 J and 1250 J, respectively (Fig. 10A). The tissue area below 0°C was used to determine the degree of cryo-anchoring present during ablation and was approximately 0.14 ± 0.05 $cm^2$ at the end of the 1250 J ablations. For comparison, the area of the cryo-anchor in contact with the leaflet during the procedure is approximately 0.12 $cm^2$. Thermal contours at the end of each treatment indicate distinct regions of cryo-anchoring and tissue ablation (Fig. 10B). The thermal contour plots at the end of the 350 J treatment shows minimal tissue > 65°C, while the majority of the leaflet tissue is > 65°C in the 1250 J treatment.

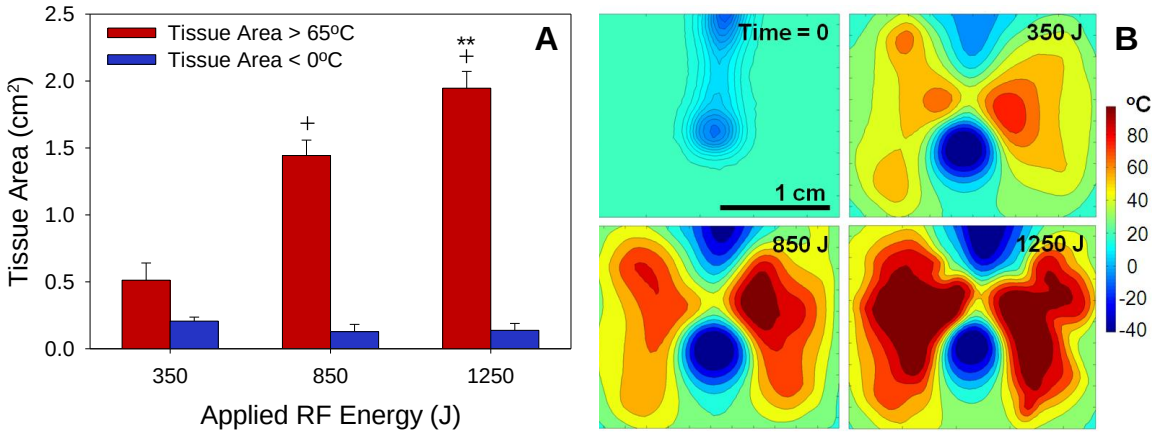


**Figure 10. Infrared Thermal Imaging.** (A) Tissue areas heated to > 65°C by RF ablation (red bars) and cooled to < 0°C by cryo-anchoring, as measured at the end of treatment. $^{+}$ Significant increase vs. 350 J ($p<0.005$) and $^{**}$ significant increase vs. 850 J ($p<0.05$). (B) Infrared thermal contour images prior to (time = 0) and following RF ablations of 350 J, 850 J, and 1250 J RF, with simultaneous cryo-anchoring.

*Anchor Strength*

Following cryo-anchoring for 10 s, anchor strength was found to be 1020 ± 23 kPa (Fig. 11). As expected, application of RF ablation at 50 W for 10 s with cryo-anchoring reduced the anchor strength significantly ($p<0.005$) to 668 ± 79 kPa; however, the adherence is still robust.

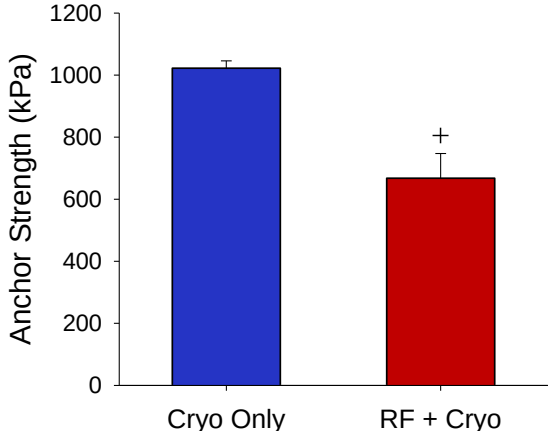


**Figure 11. Cryo-Anchor Strength.** Cryo-anchor strength following 10 s of attachment (blue bar) and 10 s of cryo-anchoring with 50 W of RF ablation (red bar). $^{+}$ Significant decrease vs. cryo only ($p<0.005$).

## Discussion

We have previously shown that RF ablation directionally alters MV leaflet geometry and compliance.[36] The therapeutic effect of our percutaneous treatment strategy is to restore competence to diseased or prolapsed MV leaflets by reducing leaflet size, and therefore, displacement of leaflets into the atrium during systole. However, any device that aims to percutaneously treat MVP must do so in a highly dynamic mechanical environment. Additionally, due to the high rate of blood flow across the MV and the resulting potential for heat convection, application of RF energy must be performed with the RF electrode in direct contact with the target tissue. Thus, we have introduced cryo-anchoring as a means to potentially maintain direct catheter contact with a moving MV leaflet and to enhance stability during the procedure. During cryo-anchoring, tissue is cooled to < 0°C, which interferes with the resistive heating that is the therapeutic mechanism behind RF ablation. However, due to the small size of MV leaflets, cryo-anchoring must be utilized in close proximity to the RF electrode. In this study, we demonstrate the effects of using two competing energy modalities and the feasibility of RF ablation performed with cryo-anchoring.

### *More RF Energy Required with Cryo-Anchoring*

Biaxial mechanical data following treatment with the catheter prototype demonstrates that RF ablation remains a valid therapy, even with sub-freezing temperatures on the cryo-anchor in close proximity on the MV leaflet (Fig. 9). To determine the extent to which cryo-anchoring reduces the biomechanical effects of RF ablation, we re-analyzed previous biaxial data from treatment with a commercially available RF catheter (7F, Blazer II, Boston Scientific) without cryo-anchoring,[36] plotting the % change in areal systolic deformation alongside our data presented here (Fig. 12). While RF ablation with cryo-anchoring altered unloaded MV leaflet geometry and

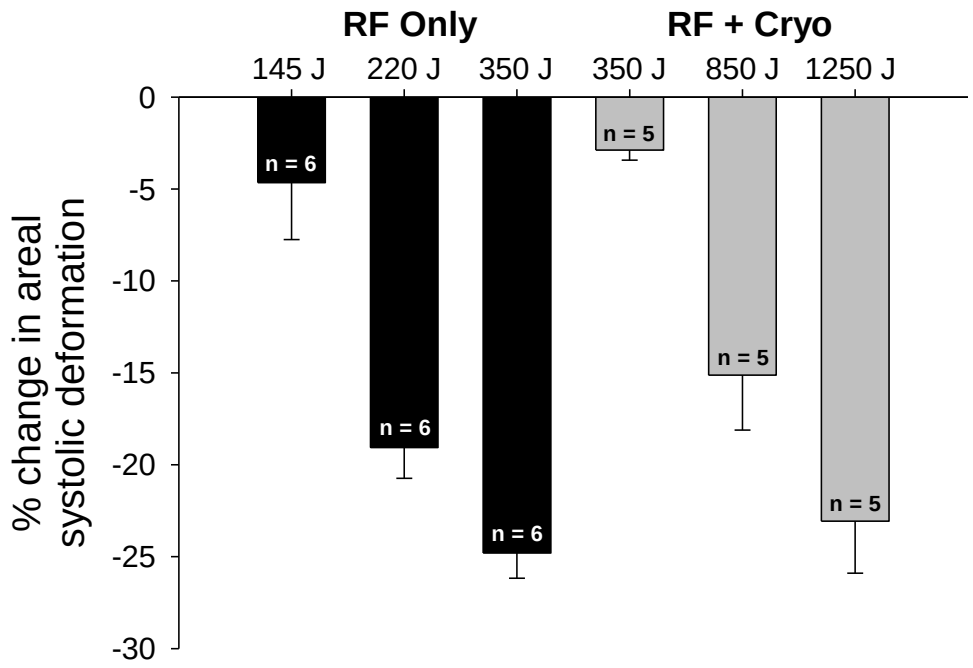


**Figure 12. Biomechanical Changes With and Without Cryo-Anchoring.** % change in areal systolic deformation with RF ablation alone (black bars) [36] and RF + cryo-anchoring (gray bars), demonstrating that more RF energy is needed when cryo-anchoring is utilized to produce the same therapeutic effect as RF ablation alone.

deformation at systolic loading, it took significantly more energy versus RF ablation alone to produce the same effect. Previous treatments using the commercially available RF catheter reduced areal systolic deformation by approximately 25% when 350 J of energy was applied at a power of 25 W.[36] In treatments utilizing cryo-anchoring, areal systolic deformation decreased by only 2.8 ± 0.6% under the same RF conditions. However, when 1250 J of energy was applied at a power of 50 W, our catheter prototype was able to produce changes similar to the commercially available catheter at 350 J. These results indicate that even though RF power must be increased significantly when cryo-anchoring is used, the catheter prototype can still achieve the same therapeutic effect.

*Thermally-Related Collagen Contracture*

RF ablation introduces both geometric and biomechanical changes in MV leaflets; specifically, changes in areal systolic deformation are primarily due to length changes in the circumferential direction (Fig. 9D). This shortening of the collagen fibers in the circumferential direction is due to thermal rupture of heat-sensitive bonds and uncoiling of the collagen triple helix. This uncoiling of collagen fibers and transition from a crystalline state to a random coil is responsible for collagen shortening, and transmission electron microscopy of collagenous tissues treated with RF ablation show collagen fibrils that increase in average diameter with increasing RF power.[30] Additionally, aligned collagen fibers fuse together in the orthogonal directions after treatment with RF ablation,[29-30] leading to modest changes seen in the radial direction here (Fig. 9D). Therefore, the use of a cryo-anchor for stability during the RF ablation procedure reduces the therapeutic effect of RF energy, but this effect can be mitigated by increasing RF power.

*Heat Distribution of RF Ablation with Cryo-Anchoring*

In addition to determining biomechanical changes induced by RF ablation, we have analyzed the temperature distribution resulting from combined RF ablation with cryo-anchoring. Estimates for the onset of unwinding of the collagen triple helix vary and have been determined to be approximately 60°C in the bovine joint capsule[34] and 67.1°C in the bovine mitral valve.[2] Thus, we used 65°C as a threshold for permanent collagen denaturation and determined the area of tissue heated above this temperature. IR imaging reveals that while there is a distinct region of cryo-anchoring present through the full thickness of the leaflet, which stays relatively consistent across all RF energies, heating due to RF ablation dominates the leaflet temperature distribution. As a result, full

thickness temperatures < 0°C are confined to an area slightly larger than the cryo-anchor attachment area. Because thermal damage to the collagen matrix forms the basis of mechanical damage, we hypothesized that the tissue area heated above 65°C would correlate with changes in areal systolic deformation (Fig. 13). Indeed, this correlation is evident when % change in areal systolic deformation is plotted against tissue area above 65°C, demonstrating that biomechanical changes may be directly related to the amount of thermal tissue damage.

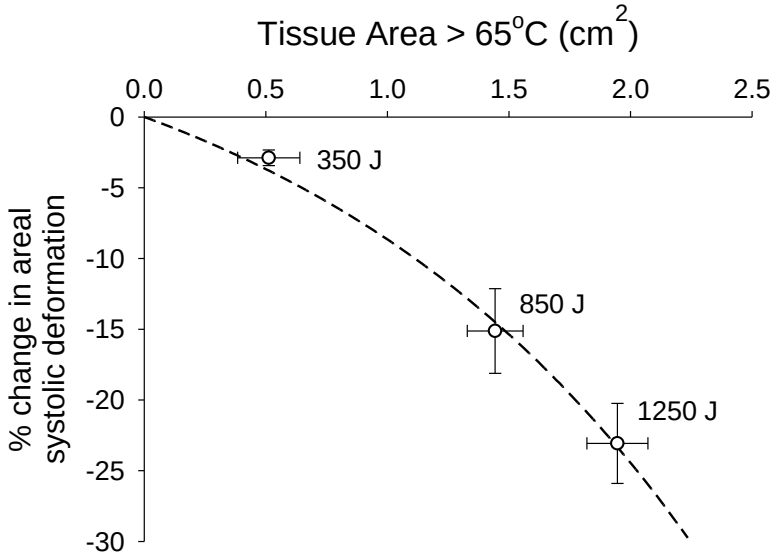


**Figure 13. Biomechanical Changes and Area of Tissue Heating.** % change in areal systolic deformation vs. tissue area > 65°C, as determined by processing of IR thermal images at the end of ablation.
Model fit: -

*Cryo-Anchor Attachment to MV Leaflets*

Testing of the anchor strength of the cryo-anchor revealed that this attachment is sufficient to maintain contact, even with RF ablation, with stationary MV leaflets. While there are currently no direct estimates for the anchor strength required to maintain attachment to the MV during the cardiac cycle, one estimate can be made based on the atrial pressure during MV opening. Because the proposed catheter treatment involves

access to the MV via the left atrium, and the peak atrial pressure is a representation of the force required to open the MV, this is an estimate for the minimum attachment force required to maintain adherence. Peak atrial pressure in normally functioning hearts is typically below 20 mmHg,[14] or about 2.7 kPa. Thus, even if a much higher estimate for the atrial pressure is chosen, this value is considerably lower than the approximately 668 kPa of anchor strength recorded at 10 s of the 50 W RF ablation. Additionally, we speculate that cryo-anchoring and ablation of MV leaflets will occur with the MV kept partially open, with one leaflet kept anchored and the other moving freely. This may further reduce the force required to maintain cryo-anchoring.

*Study Limitations*

The data presented here indicate that RF ablation performed with cryo-anchoring alters MV leaflet geometry and deformation *in vitro*; however, there are several limitations to this study. First, all treatments were performed on stationary leaflets *in vitro*. While this ensures robust delivery of RF energy, it is not realistic, particularly with regards to the anchor strength studies. Further work must be performed to verify the feasibility of cryo-anchoring on moving MV leaflets, both *in vitro* and *in vivo*. Additionally, ablations in the biomechanical and thermal imaging studies were performed on leaflets with the saline bath lowered, such that the maximum amount of RF energy would penetrate the leaflets. This provides a much more accurate measurement of the total energy delivered to the leaflet, but the *in vivo* environment is much more dynamic. Due to convective blood flow, *in vivo* treatments will require additional or prolonged RF energy delivery in order to produce the same biomechanical alterations, as demonstrated in a feasibility study utilizing a canine model.[43] Finally, these studies were performed on healthy porcine MV leaflets. It is unknown how leaflets with MVP might respond to RF ablation, due to their disorganized collagen architecture.

*Design Considerations for In Vivo Translation*

In light of the results from this study, and what is previously known regarding RF ablation, we have identified several design considerations for in vivo translation of our combined RF ablation and cryo-anchoring catheter. First, we demonstrated in vitro that RF energy must be increased when used in conjunction with cryo-anchoring in order to achieve a similar therapeutic effect of RF alone. Because our biaxial mechanical analysis was performed on leaflets treated while only partially submerged, heat dissipation will likely increase when treatment is performed in vivo, due to the surrounding hemodynamic environment. Thus, RF energy delivery will likely need to be increased in a similar manner and this will likely be accomplished by increasing either RF power or application time. Similarly, through placement in a dynamic hemodynamic environment and increases in application of RF energy, cryo-anchor strength may be reduced at the current liquid nitrogen delivery protocol, and liquid nitrogen delivery may need to be increased by increasing vacuum pressure and delivery time to compensate. Also, in order to decrease the amount of RF energy lost to the blood stream, RF electrode placement can be re-designed to allow for more direct delivery to the leaflets. One possible improvement is to replace the current, singular RF electrode, which encircles the entire 360º outer circumference of the catheter shaft, with three separate RF electrodes that are approximately 120º of the circumference and are insulated from each other. By having three separate electrodes, RF energy can be delivered to the electrode in direct contact with the leaflet, ensuring that the majority of RF energy enters the leaflet, as opposed to the bloodstream. These, and other potential modifications, will likely be necessary to translate this strategy into an integrated catheter that will be successful in vivo.

*Conclusions*

In this study, we demonstrate that RF ablation with a cryo-anchor may provide an alternative percutaneous treatment strategy for MVP. While it was previously shown that RF ablation alone reduces MV leaflet size, we have demonstrated the feasibility of cryo-anchoring as a stability technique for secure attachment of a catheter to a MV leaflet. Additionally, cryo-anchoring may have possible uses in other applications involving RF ablation or in more general percutaneous catheters as a mechanism to enhance stability and improve catheter contact in complex anatomies or hard-to-reach sites. Cryo-anchoring may be a particularly effective strategy in improving catheter stability during treatment of cardiac arrhythmias, given the dynamic environment of the heart. While we found here that cryo-anchoring reduces the effect of RF ablation, these effects can be mitigated by increasing RF power and duration. These *in vitro* results indicate that RF ablation with simultaneous cryo-anchoring reduces MV leaflet size and may be a viable clinical strategy for percutaneous treatment of myxomatous MVP.

Acknowledgments

This work was funded by the Wallace H. Coulter Foundation. The authors thank Drs. E. Duco Jansen and Mark Mackanos for use of and assistance with the IR camera.

# CHAPTER III

## CONCLUSIONS AND FUTURE WORK

### Conclusions

The result from this work is a demonstration of the feasibility of RF ablation with cryo-anchoring to reduce MV leaflet size. Additionally, this geometric shrinkage is maintained throughout the loading cycle, indicating a reduction in leaflet size at maximum systolic load when leaflets should be fully closed and without mitral regurgitation. Infrared thermal imaging revealed the feasibility of using radiofrequency ablation with cryo-anchoring in close proximity, on the same leaflet, and anchor strength demonstrated that cryo-anchor strength remains robust during application of RF energy.

### Future Work

Feasibility of the combined radiofrequency ablation and cryo-anchoring approach has been demonstrated *in vitro* on stationary, excised MV leaflets. While this represents a substantial step forward, this approach has yet to be tested on a moving, functioning mitral valve and is an important milestone before *in vivo* animal testing can begin. The first step towards testing on whole, functioning mitral valves is to use the results of these experiments to develop a new catheter prototype that can be used for further *in vitro* testing, as well as *in vivo* testing in the future. The current prototype is large and bulky, with many components – including the RF electrode and thermocouple wires – housed external to the catheter. Including these components inside the lumen of the catheter will enhance the range of tests which can be performed. Additionally, liquid nitrogen is currently pumped out of a cryo canister under a laboratory house vacuum, which limits

the length of the catheter and limits its mobility. Improving the pumping system used to deliver liquid nitrogen to the catheter tip will improve its range and enhance control over the amount of liquid nitrogen delivery.

Once these improvements have been made to the catheter prototype, further *in vitro* experiments can be performed on whole, intact mitral valves. A left heart flow simulator is currently being developed to replicate blood flow through the left side of the heart (Fig. 14).

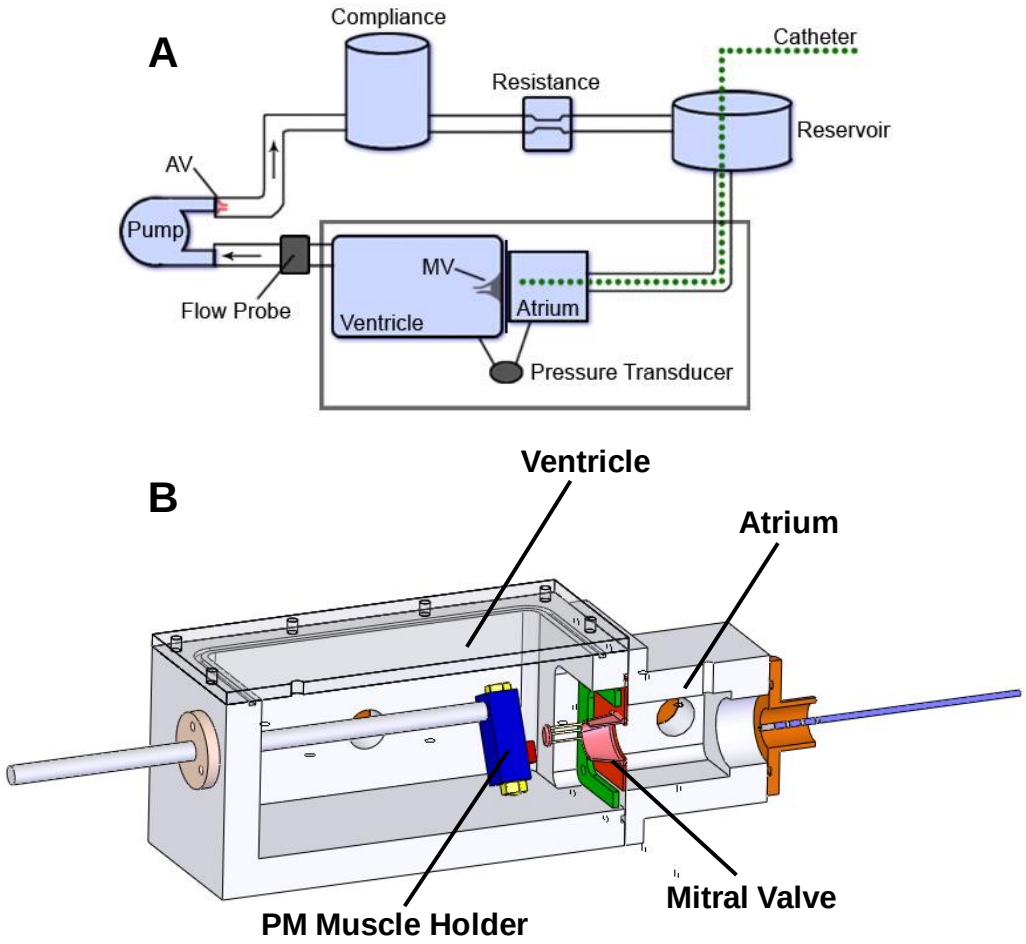


**Figure 14. Left Heart Flow Simulator Design.** A) Schematic representation of the left heart flow simulator currently in development showing the flow probe and pressure transducer to measure performance of an excised, porcine mitral valve following treatment with catheter prototypes. B) Solid model of the ventricle and atrium, showing attachment of excised mitral valves and catheter entry.

The left heart flow simulator has the capability to integrate excised porcine mitral valves within the device by suturing the mitral annulus to a flexible membrane at the ventricle-atrium interface and attaching the papillary muscles to adjustable holders within the ventricle (Fig. 15).

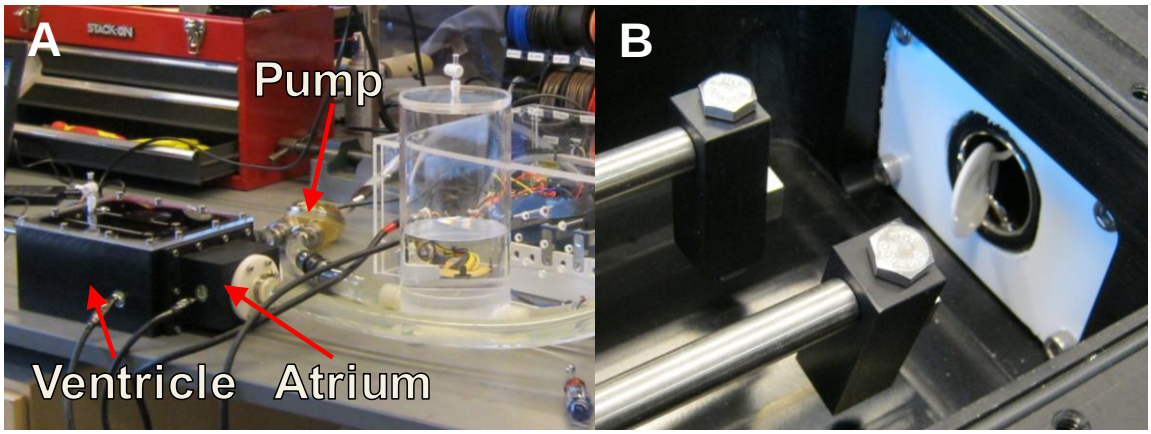


**Figure 15. Left Heart Flow Simulator Testing.** A) Testing of the left heart flow simulator, indicating placement of the ventricle, atrium, and pump. B) Papillary muscle holders and a mechanical valve indicating the attachment site for excised porcine mitral valves.

The ability to place an intact, excised MV inside a left heart simulator will allow direct measurement of changes to pressure and flow across the MV as a result of treatment with combined RF ablation and cryo-anchoring prototypes. The use of the left heart flow simulator will allow testing of catheter prototypes and refinement of control over RF energy and cryo-anchor delivery in a well-controlled environment that mimics the hemodynamics of the heart. Testing with the left heart flow simulator will provide feedback on the efficacy of catheter prototypes that will be used to improve catheter design and determine the ideal treatment protocols prior to *in vivo* animal testing. The ultimate goal of this bench-top strategy is to further validate the feasibility of combined RF ablation and cryo-anchoring as a technique to percutaneously treat MVP and to

determine the therapeutic window of treatment with RF energy prior to testing in an animal model.

## REFERENCES


1. Mitral Valve Prolapse: http://www.nlm.nih.gov/medlineplus. MedLine Plus.

2. Aldous, I. G., S. P. Veres, A. Jahangir, and J. M. Lee. Differences in collagen cross-linking between the four valves of the bovine heart: a possible role in adaptation to mechanical fatigue. Am J Physiol-Heart C. 296(6):H1898-H1906, 2009.

3. Alfieri, O., M. De Bonis, E. Lapenna, T. Regesta, F. Maisano, L. Torracca, and G. La Canna. "Edge-to-edge" repair for anterior mitral leaflet prolapse. Semin Thorac Cardiovasc Surg. 16(2):182-187, 2004.

4. Alfieri, O., F. Maisano, and A. Colombo. Future of transcatheter repair of the mitral valve. Am J Cardiol. 96(12A):71L-75L, 2005.

5. Barber, J. E., F. K. Kasper, N. B. Ratliff, D. M. Cosgrove, B. P. Griffin, and I. Vesely. Mechanical properties of myxomatous mitral valves. J Thorac Cardiovasc Surg. 122(5):955-962, 2001.

6. Chiam, P. T., and C. E. Ruiz. Percutaneous transcatheter mitral valve repair: a classification of the technology. JACC Cardiovasc Interv. 4(1):1-13, 2011.

7. Cole, W. G., D. Chan, A. J. Hickey, and D. E. Wilcken. Collagen composition of normal and myxomatous human mitral heart valves. Biochem J. 219(2):451-460, 1984.

8. Devereux, R. B., E. C. Jones, M. J. Roman, B. V. Howard, R. R. Fabsitz, J. E. Liu, V. Palmieri, T. K. Welty, and E. T. Lee. Prevalence and correlates of mitral valve prolapse in a population-based sample of American Indians: the Strong Heart Study. Am J Med. 111(9):679-685, 2001.

9. Fedak, P. W., P. M. McCarthy, and R. O. Bonow. Evolving concepts and technologies in mitral valve repair. Circulation. 117(7):963-974, 2008.

10. Feldman, T., E. Foster, D. D. Glower, S. Kar, M. J. Rinaldi, P. S. Fail, R. W. Smalling, R. Siegel, G. A. Rose, E. Engeron, C. Loghin, A. Trento, E. R. Skipper, T. Fudge, G. V. Letsou, J. M. Massaro, and L. Mauri. Percutaneous repair or surgery for mitral regurgitation. N Engl J Med. 364(15):1395-1406, 2011.

11. Feldman, T., H. S. Wasserman, H. C. Herrmann, W. Gray, P. C. Block, P. Whitlow, F. St Goar, L. Rodriguez, F. Silvestry, A. Schwartz, T. A. Sanborn, J. A. Condado, and E. Foster. Percutaneous mitral valve repair using the edge-to-

edge technique: six-month results of the EVEREST Phase I Clinical Trial. J Am Coll Cardiol. 46(11):2134-2140, 2005.

12. Freed, L. A., E. J. Benjamin, D. Levy, M. G. Larson, J. C. Evans, D. L. Fuller, B. Lehman, and R. A. Levine. Mitral valve prolapse in the general population: the benign nature of echocardiographic features in the Framingham Heart Study. J Am Coll Cardiol. 40(7):1298-1304, 2002.

13. Freed, L. A., D. Levy, R. A. Levine, M. G. Larson, J. C. Evans, D. L. Fuller, B. Lehman, and E. J. Benjamin. Prevalence and clinical outcome of mitral-valve prolapse. N Engl J Med. 341(1):1-7, 1999.

14. Fuster, V., and J. W. Hurst. Hurst's the Heart. New York: McGraw-Hill, 2004.

15. Galloway, A. C., E. A. Grossi, C. S. Bizekis, G. Ribakove, P. Ursomanno, J. Delianides, F. G. Baumann, F. C. Spencer, and S. B. Colvin. Evolving techniques for mitral valve reconstruction. Ann Surg. 236(3):288-293; discussion 293-284, 2002.

16. Goel, R., T. Witzel, D. Dickens, P. A. Takeda, and R. R. Heuser. The QuantumCor device for treating mitral regurgitation: an animal study. Catheter Cardiovasc Interv. 74(1):43-48, 2009.

17. Grashow, J. S., M. S. Sacks, J. Liao, and A. P. Yoganathan. Planar biaxial creep and stress relaxation of the mitral valve anterior leaflet. Ann Biomed Eng. 34(10):1509-1518, 2006.

18. Grashow, J. S., A. P. Yoganathan, and M. S. Sacks. Biaixal stress-stretch behavior of the mitral valve anterior leaflet at physiologic strain rates. Ann Biomed Eng. 34(2):315-325, 2006.

19. Hansen, D. E., P. D. Cahill, W. M. DeCampli, D. C. Harrison, G. C. Derby, R. S. Mitchell, and D. C. Miller. Valvular-ventricular interaction: importance of the mitral apparatus in canine left ventricular systolic performance. Circulation. 73(6):1310-1320, 1986.

20. Heuser, R. R., T. Witzel, D. Dickens, and P. A. Takeda. Percutaneous treatment for mitral regurgitation: the QuantumCor system. J Interv Cardiol. 21(2):178-182, 2008.

21. Huang, S. K. S., and M. A. Wood. Catheter Ablation of Cardiac Arrhythmias. Philadelphia: Elsevier, 2006.

22. Humphrey, J. D. Cardiovascular Solid Mechanics : Cells, Tissues, and Organs. New York: Springer, 2002.

23. Jimenez, J. H., J. Forbess, L. R. Croft, L. Small, Z. He, and A. P. Yoganathan. Effects of annular size, transmitral pressure, and mitral flow rate on the edge-to-edge repair: an in vitro study. Ann Thorac Surg. 82(4):1362-1368, 2006.

24. Khairy, P., A. Rodriguez-Santiago, M. Talajic, and E. al. Catheter cryoablation in man: Early clinical experience. The Canadian Journal of Cardiology. 15(173D), 1999.

25. King, B. D., M. A. Clark, N. Baba, J. W. Kilman, and C. F. Wooley. "Myxomatous" mitral valves: collagen dissolution as the primary defect. Circulation. 66(2):288-296, 1982.

26. Libby, P., and E. Braunwald. Braunwald's heart disease : a textbook of cardiovascular medicine. Philadelphia: Saunders/Elsevier, 2008.

27. Lim, C. B., R. D. Goldin, D. S. Elson, A. Darzi, and G. B. Hanna. In vivo thermography during small bowel fusion using radiofrequency energy. Surg Endosc. 24(10):2465-2474, 2010.

28. Lis, Y., M. C. Burleigh, D. J. Parker, A. H. Child, J. Hogg, and M. J. Davies. Biochemical characterization of individual normal, floppy and rheumatic human mitral valves. Biochem J. 244(3):597-603, 1987.

29. Lopez, M. J., L. A. DeTemple, Y. Lu, and M. D. Markel. The effects of monopolar radiofrequency energy on intact and lacerated ovine menisci. Arthroscopy. 17(6):613-619, 2001.

30. Lopez, M. J., K. Hayashi, G. S. Fanton, G. Thabit, and M. D. Markel. The effect of radiofrequency energy on the ultrastructure of joint capsular collagen. Arthroscopy. 14(5):495-501, 1998.

31. Maisano, F., G. La Canna, A. Colombo, and O. Alfieri. The evolution from surgery to percutaneous mitral valve interventions: the role of the edge-to-edge technique. J Am Coll Cardiol. 58(21):2174-2182, 2011.

32. McAfee, M. K., and H. V. Schaff. Valve Repair for Mitral Insufficiency. Cardiology. 20:35-43, 1990.

33. Medvecky, M. J., B. C. Ong, A. S. Rokito, and O. H. Sherman. Thermal capsular shrinkage: Basic science and clinical applications. Arthroscopy. 17(6):624-635, 2001.

34. Naseef, G. S., 3rd, T. E. Foster, K. Trauner, S. Solhpour, R. R. Anderson, and B. Zarins. The thermal properties of bovine joint capsule. The basic science of laser- and radiofrequency-induced capsular shrinkage. Am J Sports Med. 25(5):670-674, 1997.

35. Otto, C. M. Clinical practice. Evaluation and management of chronic mitral regurgitation. N Engl J Med. 345(10):740-746, 2001.

36. Price, S., C. Norwood, J. Williams, H. McElderry, and W. D. Merryman. Radiofrequency Ablation Directionally Alters Geometry and Biomechanical Compliance of Mitral Valve Leaflets: Refinement of a Novel Percutaneous Treatment Strategy. Cardiovascular Engineering and Technology. 1(3):194-201, 2010.

37. Rabkin, E., M. Aikawa, J. R. Stone, Y. Fukumoto, P. Libby, and F. J. Schoen. Activated interstitial myofibroblasts express catabolic enzymes and mediate matrix remodeling in myxomatous heart valves. Circulation. 104(21):2525-2532, 2001.

38. Sacks, M. S., Z. He, L. Baijens, S. Wanant, P. Shah, H. Sugimoto, and A. P. Yoganathan. Surface strains in the anterior leaflet of the functioning mitral valve. Ann Biomed Eng. 30(10):1281-1290, 2002.

39. Savage, E. B., T. B. Ferguson, Jr., and V. J. DiSesa. Use of mitral valve repair: analysis of contemporary United States experience reported to the Society of Thoracic Surgeons National Cardiac Database. Ann Thorac Surg. 75(3):820-825, 2003.

40. Skanes, A. C., G. Klein, A. Krahn, and R. Yee. Cryoablation: potentials and pitfalls. J Cardiovasc Electrophysiol. 15(10 Suppl):S28-34, 2004.

41. Trichon, B. H., G. M. Felker, L. K. Shaw, C. H. Cabell, and C. M. O'Connor. Relation of frequency and severity of mitral regurgitation to survival among patients with left ventricular systolic dysfunction and heart failure. Am J Cardiol. 91(5):538-543, 2003.

42. Victal, O. A., J. R. Teerlink, E. Gaxiola, A. W. Wallace, S. Najar, D. H. Camacho, A. Gutierrez, G. Herrera, G. Zuniga, F. Mercado-Rios, and M. B. Ratcliffe. Left ventricular volume reduction by radiofrequency heating of chronic myocardial infarction in patients with congestive heart failure. Circulation. 105(11):1317-1322, 2002.

43. Williams, J. L., Y. Toyoda, T. Ota, D. Gutkin, W. Katz, M. Zenati, and D. Schwartzman. Feasibility of myxomatous mitral valve repair using direct leaflet and chordal radiofrequency ablation. J Interv Cardiol. 21(6):547-554, 2008.

44. Wood, M., S. Goldberg, M. Lau, A. Goel, D. Alexander, F. Han, and S. Feinstein. Direct measurement of the lethal isotherm for radiofrequency ablation of myocardial tissue. Circ Arrhythm Electrophysiol. 4(3):373-378, 2011.

45. www.bioethics.gov. The President's Council on Bioethics.309, 2005.

46. Yun, K. L., M. A. Niczyporuk, G. E. Sarris, J. I. Fann, and D. C. Miller. Importance of mitral subvalvular apparatus in terms of cardiac energetics and systolic mechanics in the ejecting canine heart. J Clin Invest. 87(1):247-254, 1991.